Reflectivity cross plot of Modified Zoeppritz Equation

ABSTRACT

Beside the complexities and not readily practical applications resulting from the full Zoeppritz equation, the seismic amplitude reflection does not give enough information beyond the critical angle. Consequently, there are breakdown of the Zoeppritz equation approximations at angle of incidence beyond 30° (Shuey's approximation). More so, the validity is only for slight contrast in elastic parameters across the formations and small angle of incidence is assumed. In an attempt to address these inaccuracies and enhance understanding of seismic reservoir responses and prediction of fluid and lithology, a modified form of the Zoeppritz equation is derived using relations between elastic constants and velocities in terms of Pseudo Poisson' ratio reflectivity, rigidity reflectivity, density reflectivity in linearized forms devoid of the complexities associated with the original Zoeppritz equation with practical applications in hydrocarbon exploration, exploitation and production. These properties are lithology and fluid discriminators.The modified Zoeppritz equation was analyzed using well data from oil field in a sedimentary basin, onshore of Niger Delta area. Reflectivity crossplot was carried out and comparison with the exact and other approximations was done to validate the derived equation. The results showed that the modified equation can be applied in exploration beyond the critical angle than the shuey's and Aki & Richards' approximations especially for deep targets and wide angle acquisition for accurate estimation of intercept and gradient attributes. The modified Zoeppritz equation in this study gives higher accuracy at far offset than the two foremost approximations.

Keywords: Zoeppritz Equation, Aki & Richards' approximation, Shuey's approximationPseudo Poisson' ratio reflectivity,rigidity reflectivity, density reflectivity, Reflectivity crossplot

1. INTRODUCTION

The Zoeppritz equations are complicated, complex and non-linear that an intuitive understanding of how the variations of amplitude are related to different rock properties was not readily apparent [1]. Through the years, some linearized approximations to the Zoeppritz equations had been made, which make the interpretation extra intuitive [2].

A number of modifications to the full Zoeppritz equation that have been linearized can be reviewed based on their different emphasis. Starting from the equation of [3], which emphasis are on the fluid and rigidity properties, providing insight to fluid substitution interpretation. [4] looked at the contrast in the compressional (P-wave) and Shear (S- wave)

velocities and density, while [5] relates the amplitude contrast to changes in Poisson's ratio, compressional (P-wave) velocity, and density [6]. The Primary wave and Secondary wave velocity reflectivities were deduced from the equation given by [7] from which they derived the fluid factor [6, 8]. [9]gives us a direct estimation of P-wave impedance and S-wave impedance, based on which [10] proposed Lambda –Mu-Rho (LMR) method and in 1995, [11] approximation was used to derive P-wave reflectivity and Poisson's reflectivity. The equation from [12] was use for the extraction of Lambda reflectivity $\Delta\lambda/\lambda$, Mu reflectivity $\Delta\mu/\mu$, and bulk modulus reflectivity $\Delta K/K$, and the lead to [13] given an approximation to take care of the inaccuracy of the V_s/V_pratio which affects the inversion process in [12]. This study aims at modifying and analyzing Zoeppritz Equation to enhance characterization of lithology and discrimination of fluid in a typical Niger delta hydrocarbon reservoir terms of shear modulus, Psuedo-Poisson's ratio, and density with the generation of reflectivity curves for incidence angles 0^0 to 90^0 to validate the modified equation.

1.1 Zoeppritz equation

The Zoeppritz equation expresses the reflected compressional (P-wave) and shear (S-wave) with that of the transmitted compressional (P-wave) and shear (S-wave) amplitudes when a primary wave strikes the interface between two elastic media. The corresponding coefficients of reflectivity and transmissivity are dependent on the incident angle and on the material of elastic parameters of both layers [14].

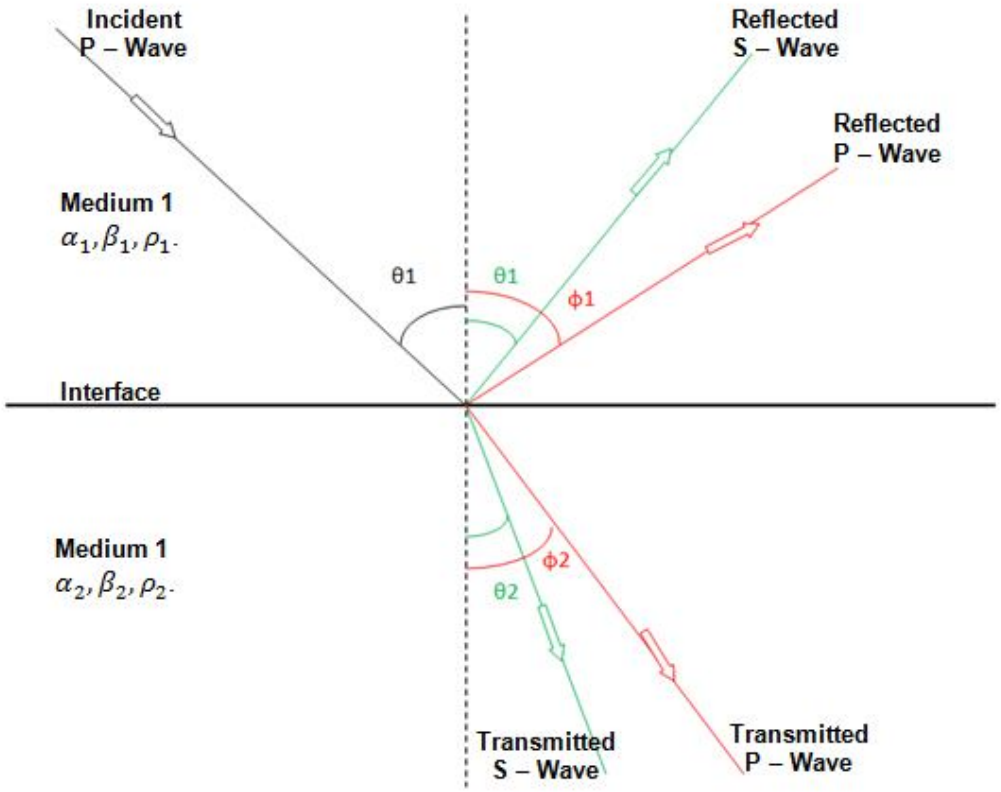

Fig. 1.Reflection and transmission at an interface between two infinite elastic half-spaces for an incident P-wave [15,16].

The resulting Zoeppritz equations for the P-P reflectivity amplitude and P-S reflectivity amplitude from the partitioning of energy between the reflected and transmitted P-waves and S-waves on either side of the interface is given as:

$$R_{PP} = \left[\left(b\frac{cos\theta_1}{\alpha_1} - c\frac{cos\theta_2}{\alpha_2}\right)F - \left(a + d\frac{cos\theta_1}{\alpha_1}\frac{cos\phi_1}{\beta_1}\right)Hp^2\right]/D \quad 1$$

$$R_{PS} = -2\frac{cos\theta_1}{\alpha_1}\left(ab + cd\frac{cos\theta_2}{\alpha_2}\frac{cos\phi_2}{\beta_2}\right)p\alpha_1/(\beta_1 D) \quad 2$$

where

$a = \rho_2(1-2\beta_2^2p^2) - \rho_1(1-2\beta_1^2p^2)$,

$b = \rho_2(1-2\beta_2^2p^2) + 2\rho_1\beta_1^2p^2$,

$c = \rho_1(1-2\beta_1^2p^2) + 2\rho_2\beta_2^2p^2$,

$d = 2(\rho_2\beta_2^2 - \rho_1\beta_1^2)$,

$E = b\frac{cos\theta_1}{\alpha_1} + c\frac{cos\theta_2}{\alpha_2}$,

$F = b\frac{cos\phi_1}{\beta_1} + c\frac{cos\phi_2}{\beta_2}$,

$G = a - d\frac{cos\theta_1}{\alpha_1}\frac{cos\phi_2}{\beta_2}$,

$H = a - d\frac{cos\theta_2}{\alpha_2}\frac{cos\phi_1}{\beta_1}$, and$D = EF + GHp_2 = (detA)/(\alpha_1\alpha_2\beta_1\beta_2)$

The difference in velocities and densities (compressional-wave velocity(α), shear –wave velocity(β) and density(ρ), with the subscripts denoting the layer number) between the first and second layers cause the angle (θ_1) of reflected P-wave energy to differ from the angle (θ_2) of transmitted P-wave energy. Similarly, the angle (ϕ_1) of incident S-wave energy is not the same as the angle (ϕ_2) of transmitted S-wave energy (Figure 1).

1.2 AKI-RICHARDS-FRASIER APPROXIMATION

The approximation of Zoeppritz equation for P-P reflectivity amplitude was firstly reformulation by[3] by making it simpler to understand the dependence of the reflection amplitudes on the angle of incident and physical properties which emphasis on the fluid and rigidity term [17].

$$R(\theta_1) = \frac{1}{2}ln\left(\frac{V_{P2}\rho_2 cos\theta_2}{V_{P1}\rho_1 cos\theta_1}\right) + \left(2 + \frac{ln\left(\frac{\rho_2}{\rho_1}\right)}{ln\left(\frac{V_{P2}}{V_{P1}}\right) - ln\left(\frac{V_{P2}V_{S1}}{V_{P1}V_{S2}}\right)}\right)\frac{V_{S1}^2 - V_{S2}^2}{V_{P1}^2}sin^2\theta_1 \quad 3$$

Bortfeld's approximation was reformulated by [18], then later by [4]. The Aki-Richards-Frasier modification is comprised of three different terms, the very first term involving P-wave velocity, the second term involving S-wave velocity, and density the third term [2]. Their approximation can be written as:

$$R(\theta) = \left[\frac{1}{2}(1 + \tan^2\theta)\right]\frac{\Delta V_P}{V_P} - \left[4\frac{V_S^2}{V_P^2}\sin^2\theta\right]\frac{\Delta VS}{V_S} + \left[\frac{1}{2}\left(1 - 4\frac{V_S^2}{V_P^2}\sin^2\theta\right)\right]\frac{\Delta\rho}{\rho} \quad 4$$

where$V_P = (V_{P1} + V_{P2})/2$, average P-wave velocity of the two layers, $\Delta V_P = V_{P2} - V_{P1}$, is the difference in P-wave velocities across the boundary$V_S = (V_{S1} + V_{S2})/2$, average S-wave velocity of the two layers, $\Delta V_S = V_{S2} - V_{S1}$, is the difference in S-wave velocities across the interface, $\rho = (\rho_1 + \rho_2)/2$, average density of the two layers, $\Delta\rho = \rho_2 - \rho_1$, is the difference in density across the interface and $\theta = (\theta_1 + \theta_2)/2$, average of the incident and transmitted angles for P-wave. [19] showedthe crossplot of the reflection coefficients obtained from the Zoeppritz equation and the Aki and Richards approximation, with the incident angle varying from 0° to 70° (Figure 2). The result shows that when the incident angle varies from 0° to 25°, the reflection coefficients obtained from the Zoeppritz equation and the Aki and Richards approximation fit very well [19].

The Aki-Richards-Frasier explained that the variation seen in amplitude was caused by the different variation in each of the density, primary wave velocity, and secondary wave velocity. Equation 4 gives the derivation of P-wave reflection coefficient, S-wave reflection coefficient, and density reflection coefficient [6].

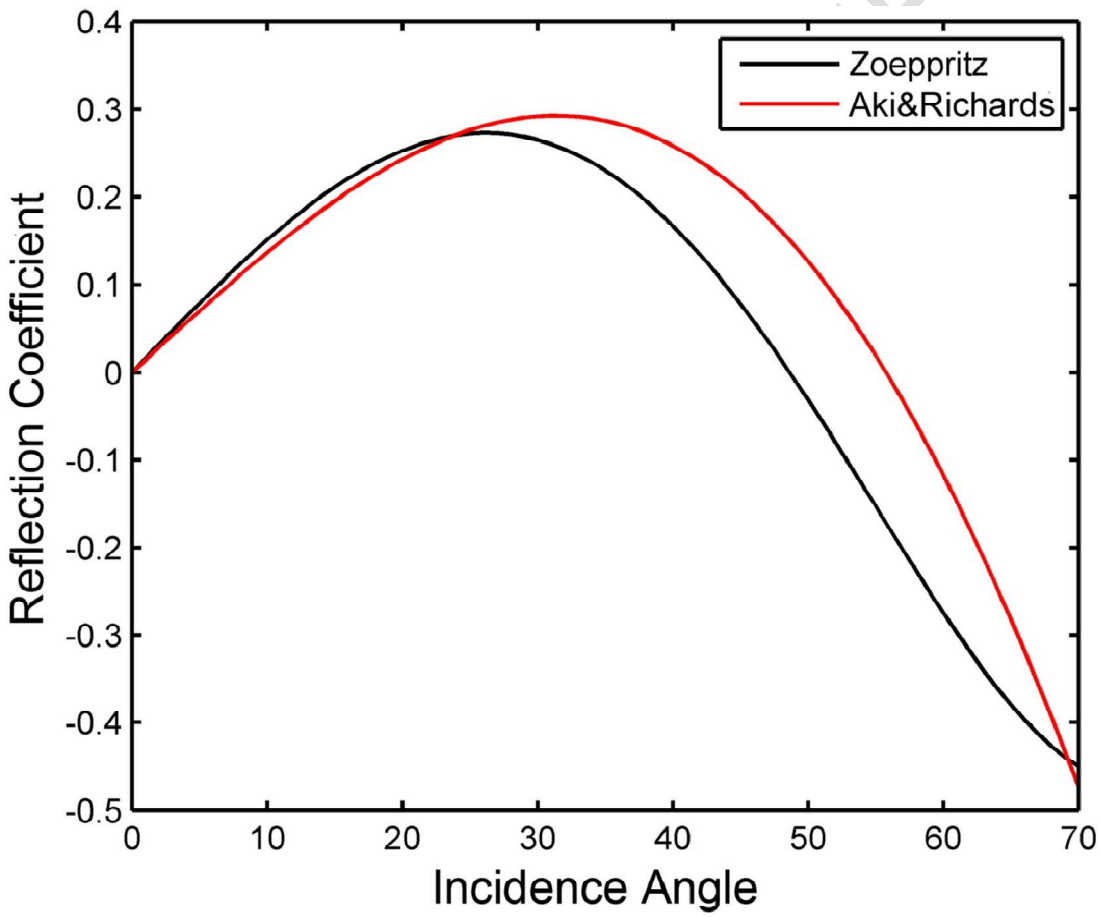

Fig. 2. Reflection coefficients obtained from Zoeppritz equation(black line) and Aki and Richards approximation (red line) [19].

1.3 SHUEY'S APPROXIMATION

The Shuey's approximation [5] gave the explicit form relating the amplitude variation to the incident angle [6]:

$$R(\theta) = \frac{1}{2}\left[\frac{\Delta V_P}{V_P} + \frac{\Delta\rho}{\rho}\right] + \left[\frac{1}{2}\frac{\Delta V_P}{V_P} - 4\left(\frac{V_S}{V_P}\right)^2\frac{\Delta V_S}{V_S} - 2\left(\frac{V_S}{V_P}\right)^2\frac{\Delta\rho}{\rho}\right]\sin^2\theta + \frac{1}{2}\frac{\Delta V_P}{V_P}(\tan^2\theta - \sin^2\theta) \quad 5$$

Afterwards, Equation 5 was rewritten by removing shear(S-wave) velocity term and putting poisson's ratio term [2]:

$$R(\theta) = \frac{1}{2}\left[\frac{\Delta V_P}{V_P} + \frac{\Delta\rho}{\rho}\right] + \left[\frac{1}{2}\frac{\Delta V_P}{V_P}\left(2\frac{\Delta V_P}{V_P} + \frac{\Delta\rho}{\rho}\right)\left(\frac{1-2\sigma}{1-\sigma}\right) + \frac{\Delta\sigma}{(1-\sigma)^2}\right]sin^2\theta + \frac{1}{2}\frac{\Delta V_P}{V_P}(tan^2\theta - sin^2\theta) \quad 6$$

According to [20] and [21] incidence at the normal represents the first termand its value depends on P-wave velocity and density contrasts. The second term, the intermediate is where characterization of R (θ) is done and it comprises one important parameter the Poisson' ratio (σ). The critical angle occurs at the third term, and according to [22], it assumes small values for the angles normally observed in reflection seismology.
Making the ratio of Shear (S-wave) to compressional (P-wave) velocityto be 0.5and the angle of incident is less than 30°(for small offsets), then neglecting the third term [17].
Equation 5 can be rewritten as:

$$R(\theta) = \frac{1}{2}\left[\frac{\Delta V_P}{V_P} + \frac{\Delta\rho}{\rho}\right] + \left[\frac{1}{2}\frac{\Delta V_P}{V_P} - \frac{\Delta V_S}{V_S} - \frac{1}{2}\frac{\Delta\rho}{\rho}\right]sin^2\theta \quad 7$$

where P-wave and S-wave reflectivity linearized are given as:

$$R_P = \frac{1}{2}\left[\frac{\Delta V_P}{V_P} + \frac{\Delta\rho}{\rho}\right], \quad \text{and} R_S = \frac{1}{2}\left[\frac{\Delta V_S}{V_S} + \frac{\Delta\rho}{\rho}\right] \quad 8$$

substitute Equations 7 and 8 into Equation 6 to get

$$R(\theta) = R_P + (R_P - 2R_S)sin^2\theta = R_P + Gsin^2\theta \quad 9$$

where, $G = R_P - 2R_S$, $R_S = \frac{R_P - G}{2}$

Considering $sin^2\theta$ as a variable, according to Equation 9, the estimation of AVO gradient G and AVO intercept R_P attributes can be performed and shear wave reflectivity R_S can be derived using the equation [6]:

$$R_S = (R_P - G)/2 \quad 10$$

Therelevant change proposed by [5]was the transformation of S-wave velocity to Poisson´s ratio with the following relationship:

$$V_S{}^2 = \frac{1}{2}\left(\frac{1-2\sigma}{1-\sigma}\right)V_p{}^2 \quad 11$$

Given that, $V_S = \frac{1}{2}(V_{S1} + V_{S2})$

Apart from [5], numerous authors such as [22, 23 24] also emphasize this relationship between the two variables (S-wave velocity and Poisson's ratio) proposed by Shuey.From [5] perspectives, Poisson's ratio is a key elastic parameter to describe the connection between the reflection coefficient and the incidence angles, and this parameter is crucial to evaluate petrophysical properties.
According to [25] crossplot of the reflection coefficients obtained from the Zoeppritz equation and the shuey'stwo-term approximation (Figure 3), with the incident angle varying from 0° to 90°for the top of a class IV (quadrant II) gas sand, and the corresponding brine-sand reflectionshows that when the incident angle varies from0° to 25°, the reflection coefficients

(even though large) obtained from theZoeppritz equation and the shuey'stwo-term approximationfit very well [25].

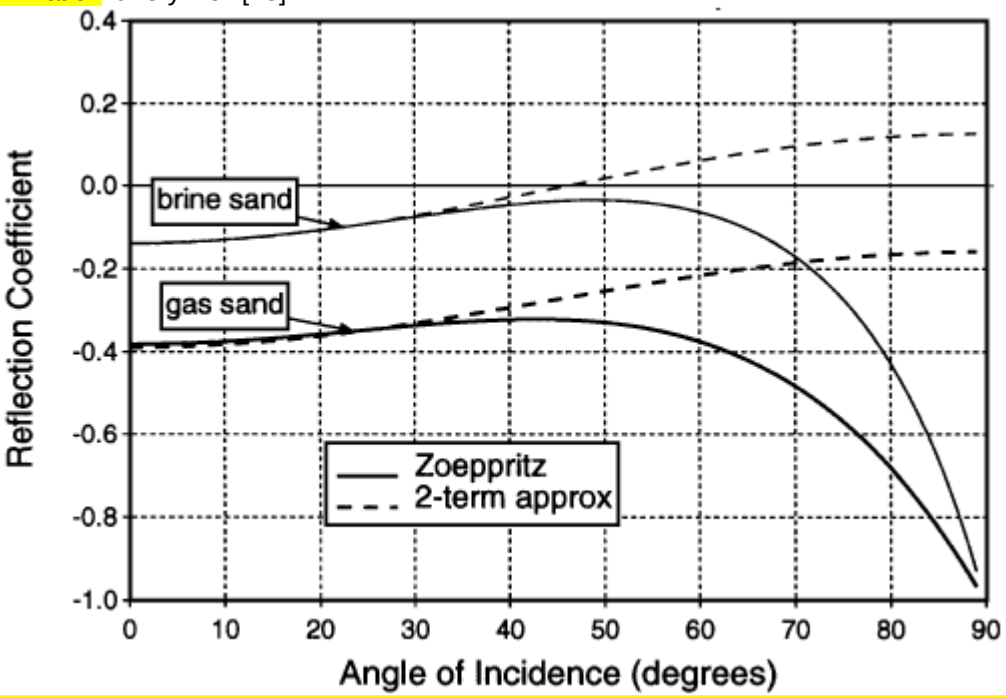

Fig. 3. Plane-wave reflection coefficient versus angle of incidence for the top of a class IV (quadrant II) gas sand, and the corresponding brine-sand reflection.The solid lines are the full Zoeppritz solution. The dashed lines are the two-term Shuey's approximation [25].

1.4 The General Linearized Approximation to Zoeppritz Equation

[26] summarized several Zoeppritz equation that was linearized based on their different emphasis into a three term equation as:

$$R(\theta) = aR_1 + bR_2 + cR_3 \qquad 12$$

$R_i$are reflectivity terms for the rock properties, the incident angle and $(V_p / V_s)^2$ are funtions of coefficients a, b, and c [6, 26]. This equation generalizes the linearized approximations and summarized in Table 1 and Table 2.

Table 1:R_i terms for the general linearized equation [6, 26]

Approximations	R_1	R_2	R_3	Assumption
Aki-Richards (1980) ($V_P V_S \rho$)	$\frac{\Delta V_P}{V_P}$	$\frac{\Delta V_S}{V_S}$	$\frac{\Delta \rho}{\rho}$	From Bortfeld's approximation
Shuey, (1985) ($\rho V_P, \sigma, V_P$)	$\frac{1}{2}\left[\frac{\Delta V_P}{V_P}+\frac{\Delta \rho}{\rho}\right]$	$\left[\frac{1}{2}\frac{\Delta V_P}{V_P}-\frac{\Delta V_S}{V_S}-\frac{1}{2}\frac{\Delta \rho}{\rho}\right]$	$\frac{1}{2}\frac{\Delta V_P}{V_P}$	The third term can be ignored for θ>30°; Assume V_S/V_p = 0.5
Smith and Gidlow (1987) ($V_P V_S \rho$)	$\frac{\Delta V_P}{V_P}$	$\frac{\Delta V_S}{V_S}$	$\frac{1}{2}\frac{\Delta V_P}{V_P}$	Gardner's relationship for density; No assumption for incident angle
Fatti et al. (1994) ($\rho V_P, \rho V_S, \rho$)	$\frac{\Delta I_P}{I_P}$	$\frac{\Delta I_S}{I_S}$	$\frac{\Delta \rho}{\rho}$	The third term can be ignored for θ>30°
Hilterman (1995) ($\rho V_P, \sigma$)	$\frac{\Delta I_P}{I_P}$	$\frac{\Delta \sigma}{(1-\sigma)^2}$	0	From Shuey's approximation Assume V_S/V_p = 0.5
Gray (1999) ($\lambda \mu \rho$)	$\frac{\Delta \lambda}{\lambda}$	$\frac{\Delta \mu}{\mu}$	$\frac{\Delta \rho}{\rho}$	No assumption
Gray (1999) ($K \mu \rho$)	$\frac{\Delta K}{K}$	$\frac{\Delta \mu}{\mu}$	$\frac{\Delta \rho}{\rho}$	No assumption
Samba and Jiangpiang (2011) ($\lambda Q \rho$)	$\frac{\Delta \lambda}{\lambda}$	$\frac{\Delta Q}{Q}=\frac{\Delta \lambda}{\lambda}-\frac{\Delta \mu}{\mu}$	$\frac{\Delta \rho}{\rho}$	From Gray's approximation Assume V_S/V_p = 0.5

Table 2: Terms a, b, and c for the general linearized equation [6, 26]

Approximations	a	b	c
Aki-Richards (1980) ($V_P V_S \rho$)	$\frac{1}{2}(1+\tan^2\theta)$	$4\frac{V_S^2}{V_P^2}\sin^2\theta$	$\frac{1}{2}\left(1-4\frac{V_S^2}{V_P^2}\sin^2\theta\right)$
Shuey, 1985 ($\rho V_P, \sigma, V_P$)	1	$\sin^2\theta$	$\tan^2\theta-\sin^2\theta$
Smith and Gidlow (1987) ($V_P V_S \rho$)	$\frac{5}{8}-1/2(V_S^2/V_P^2)sin^2\theta+1/2tan^2\theta$	$-4(V_S^2/V_P^2)sin^2\theta$	$\tan^2\theta$
Fatti et al. (1994) ($\rho V_P, \rho V_S, \rho$)	$(1+tan^2\theta)$	$-4\left(\frac{V_S}{V_P}\right)^2 sin^2\theta$	$-\left(\frac{1}{2}tan^2\theta-2\left(\frac{V_S}{V_P}\right)^2 sin^2\theta\right)$
Hilterman (1995) ($\rho V_P, \sigma$)	$cos^2\theta$	$sin^2\theta$	0
Gray (1999) ($\lambda \mu \rho$)	$\left[\frac{1}{4}-2\left(\frac{\beta}{\alpha}\right)^2\right]sec^2\theta$	$\left(\frac{\beta}{\alpha}\right)^2\left[\frac{sec^2\theta}{2}-2sin^2\theta\right]$	$\left[\frac{1}{2}-\frac{1}{4}sec^2\theta\right]$
Gray (1999) ($K \mu \rho$)	$\left[\frac{1}{4}-\frac{1}{3}\left(\frac{\beta}{\alpha}\right)^2\right]sec^2\theta$	$\left(\frac{\beta}{\alpha}\right)^2\left[\frac{sec^2\theta}{3}-2sin^2\theta\right]$	$\left[\frac{1}{2}-\frac{1}{4}sec^2\theta\right]$
Samba and Jiangpiang (2011) ($\lambda Q \rho$)	$\left[\frac{sec^2\theta}{4}-2Ksin^2\theta\right]$	$\left(\frac{\beta}{\alpha}\right)^2\left[2Ksin^2\theta-\frac{1}{2}sec^2\theta\right]$	$\frac{1}{4}[1-tan^2\theta]$

1.5 LOCATION OF THE STUDY AREA

The study area lies in a producing Niger Delta oilfield (Figure 4). It is situated in the southern part of Nigeria and characterized by mangrove and rain forest vegetation. It is characterized by high annual rainfall and temperatures almost throughout the year. The terrain is generally swampy in nature, with river channels and tributaries emptying into the Atlantic Ocean. The Niger Delta lies between longitudes 3°E - 9°E and latitudes 4°N - 6°N and is situated on the West African continental margin, where the east trending equatorial coast turns south towards the equator [27, 28].The Niger Delta is regarded one of the most prolific oil and gas provinces in the world [29].The lithostratigraphy of the Tertiary Niger Delta (Figure 5) can be separated into three distinct formations that are renowned mostly on the premise of their sand-shale ratio [30]: Benin, Agbada and Akata, formations, with depositional environments ranging from marine, transitional and continental settings respectively[30, 31, 32]. The Benin, Agbada and Akata formations lie over stretched continental and oceanic crusts [33]. Their ages range from Eocene to Recent, yet transgress time boundaries [34,35]

Fig. 4.Map of Nigeria showing the Niger Delta Complex and the study location[36].

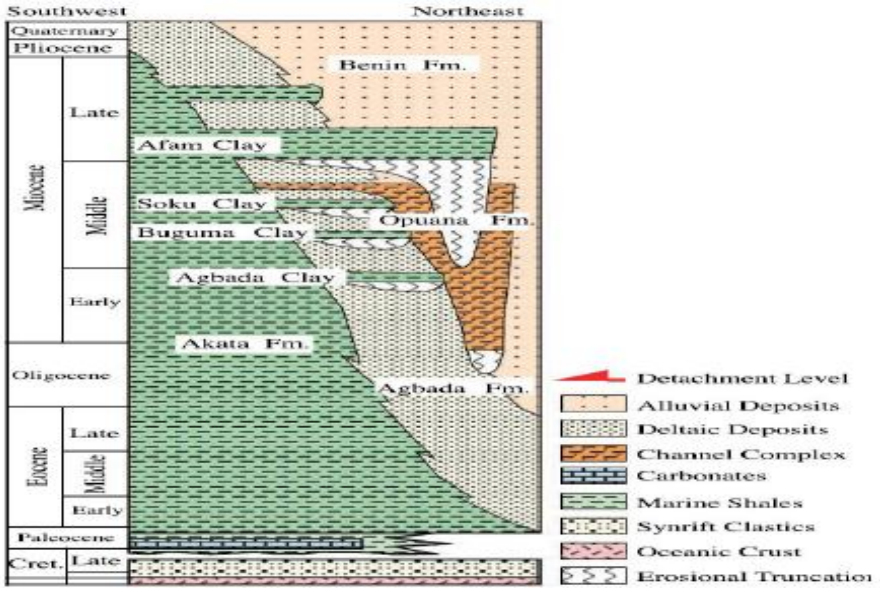

Fig.5.Regional Stratigraphy of the Niger Delta [29, 37].

2. MATERIAL AND METHODS

The materials required for the study is a well log data from a field in Niger Delta Basin. Hampson Russell (HR)Software were used for data processing, while Maple 18 Software was used for the reflectivity crossplots.
[4] equationwas rearranged in terms of Pseudo Poisson' ratio reflectivity ($\Delta q/\mathrm{q}$), rigidity reflectivity ($\Delta\mu/\mu$), and density reflectivity ($\Delta\rho/\rho$). These properties are lithology and fluid discriminators[38].

$$R_P(\theta) = \frac{1}{2}\left[\frac{\Delta V_P}{V_P} + \frac{\Delta\rho}{\rho}\right] - 2\left(\frac{V_S}{V_P}\right)^2\left[\frac{2\Delta V_S}{V_S} + \frac{\Delta\rho}{\rho}\right] sin^2\theta + \frac{1}{2}\frac{\Delta V_P}{V_P} tan^2\theta \quad 13$$

$$R_P(\theta) = \frac{1}{2}\left(\frac{\Delta V_P}{V_P} - \frac{\Delta V_S}{V_S}\right)(1 + tan^2\theta) + \frac{1}{2}\frac{\Delta V_S}{V_S}\left(sec^2\theta - 8\left(\frac{V_S}{V_P}\right)^2 sin^2\theta\right) + \frac{1}{2}\frac{\Delta\rho}{\rho}\left(1 - 4\left(\frac{V_S}{V_P}\right)^2 sin^2\theta\right) \quad 14$$

According to [2] and [39], the Pseudo Poisson's ratio is defined as:

$$\frac{\Delta q}{\mathrm{q}} \equiv \frac{\Delta(V_P/V_S)}{V_P/V_S} = \frac{\Delta(I_P/I_S)}{I_P/I_S} = \frac{\Delta V_P}{V_P} - \frac{\Delta V_S}{V_S} = \frac{\Delta I_P}{I_P} - \frac{\Delta I_S}{I_S} \quad 15$$

Therefore, substitute Equation 15 into Equation 14,

$$R_P(\theta) = \frac{1}{2}\frac{\Delta q}{q}(1 + tan^2\theta) + \frac{1}{2}\frac{\Delta V_S}{V_S}\left(sec^2\theta - 8\left(\frac{V_S}{V_P}\right)^2 sin^2\theta\right) + \frac{1}{2}\frac{\Delta\rho}{\rho}\left(1 - 4\left(\frac{V_S}{V_P}\right)^2 sin^2\theta\right) \quad 16$$

Moreso, [40] gave $\Delta\mu$as
$\Delta\mu = {V_S}^2\Delta\rho + 2\rho V_S\Delta V_S$ 17

Therefore, Equation 16 can be rewritten as

$$\boldsymbol{R_P(\theta) = \frac{1}{2}\frac{\Delta q}{q}(1 + \tan^2\theta) + \frac{1}{2}\frac{\Delta\mu}{\mu}\left(\frac{\sec^2\theta}{2} - 4\left(\frac{V_S}{V_P}\right)^2 \sin^2\theta\right) + \frac{1}{2}\frac{\Delta\rho}{\rho}\left(1 - \frac{1}{2}\sec^2\theta\right)} \quad 18$$

Equation 18 is the modified Zoeppritz equation [41, 42].

Basically, a relationship, possibly linear, between the rock physical properties (P- and S-wave velocities, Density, Impedances, Bulk Modulus, Shear Modulus, Lamé's parameter , Pseudo-Poisson ratio e.t.c) and seismic reflections, that is, the rock attributes of the formations were examined to create a relationship between the petrophysical data and elastic properties using HR software. After creating this relationship, Maple 18 software was used to generate reflectivity curves. The Exact Zeoppritz equation, Aki-Richards, Shuey and the modified Zoeppritz equation were used to generate reflectivity curves for a single interface separating two isotropic materials for an incident plane wave.

3. RESULTS AND DISCUSSION

The results of P-P reflectivity from the modified Zoeppritz equation were crossplotted against incidence angles0° – 90° and compared with the exact Zoeppritz equation and other approximations.

A comparison of results obtained from P-P reflectivity coefficient versus incident angle for shale over gas sand and shale over oil sand scenarios, using the exact Zoeppritz, Aki-Richards and modified Zoeppritz Equations of P-P reflectivity coefficient with respect to angle of incidence as shown in Figure 6

The rock properties for shale over oil sand scenario used for this plot are:

- P-wave velocities: in shale 2650 m/s, and in oil sand 2560m/s
- S-wave velocities: in shale 1150 m/s, and in oil sand 1180m/s
- Densities : in shale 2.48 g/cc , and in oil sand 2.23 g/cc

The rock properties for shale over gas sand scenario used for this plot are:

- P-wave velocities: in shale 2650 m/s, and in gas sand 2340m/s
- S-wave velocities: in shale 1150 m/s, and gas sand 1180m/s
- Densities : in shale 2.48 g/cc, and in gas sand 2.16 g/cc

Figure 6 is a plot of shale over gas sand and shale over oil sand scenarios. There are both Class III AVO responses, having normal reflectivity amplitudeR_0 negative and increases with increasing angle/offset. The AVO plot shale over gas sands response exhibit a negative zero-offset reflection coefficient (≈ -0.1311), while shale over oil sand response exhibit a negative zero- degree offset reflection coefficient (≈-0.0703).

The reflectivity for shale over gas sand is high than shale over oil sand in each of the plots. This by implication implies larger reflection amplitudes for shale over gas sand than shale over oil sand. The fit is better and well pronounced for shale over oil sand plot.

The plot shows that Zoeppritz's equation, Aki and Richard's approximation and the modified equation fit each other near the critical angle 25° while that of Zoeppritz and the modified equation fit well beyond25°. This could be attributed to the sensitivity of the elastic parameters in the modified equation which are fractional contrast ofPseudo Poisson' ratio reflectivity ($\Delta q/\mathrm{q}$), rigidity reflectivity ($\Delta\mu/\mu$), and density reflectivity ($\Delta\rho/\rho$).

A comparison of results obtained for a gas sand over shale reflection for Shuey's approximation and modified equation for P-P reflection coefficient with respect to angle of incidence as shown in Figure 7

The rock properties for gas over shale sand scenario used for this plot are:

- P-wave velocities: in gas sand 1650 m/s, in shale 3240m/s
- S-wave velocities: in gas sand 1090 m/s, in shale 1620m/s
- Densities: in gas sand 2.07 g/cm^3 , in shale 2.34 g/cm^3

The gas over shale formation in Figure 7 at zero offset starts with slightly negative reflection coefficient, it becomes less negative as the offset increases for gas over shale reflectivity generated from Shuey's equation with a phase change at less than 30°angle of incidence. On the other hand, the reflectivity generated from the modified equation increase in amplitude slightly with a phase change occurring at less than 40° angle of incidence. The Shuey's and the modified equation show the same fit at the near angle of incidence with a negative zero-offset reflection coefficient (≈-0.0983).

From the plot it was observed that the Shuey's approximation breaks down before the critical angle showing the inadequacy of the approximation while the modified equation is stable at angles above the critical angle 30°. This could be attributed to the sensitivity of the elastic parameters in the modified equation which are fractional contrast of Pseudo Poisson' ratio reflectivity ($\Delta q/\mathrm{q}$), rigidity reflectivity ($\Delta\mu/\mu$), and density reflectivity ($\Delta\rho/\rho$).Therefore, the modified equation can be used to explore at increasing angle/offset beyond the critical angle than the shuey's approximation.

The modified equation has reflectivity at increasing angle of incidence $R(\theta)$ slightly less negative than Shuey's approximation. Shuey's approximation is best at incident angle less than 30°, while the modified equation is best at incident angle less than 60° before the second phase reversal.

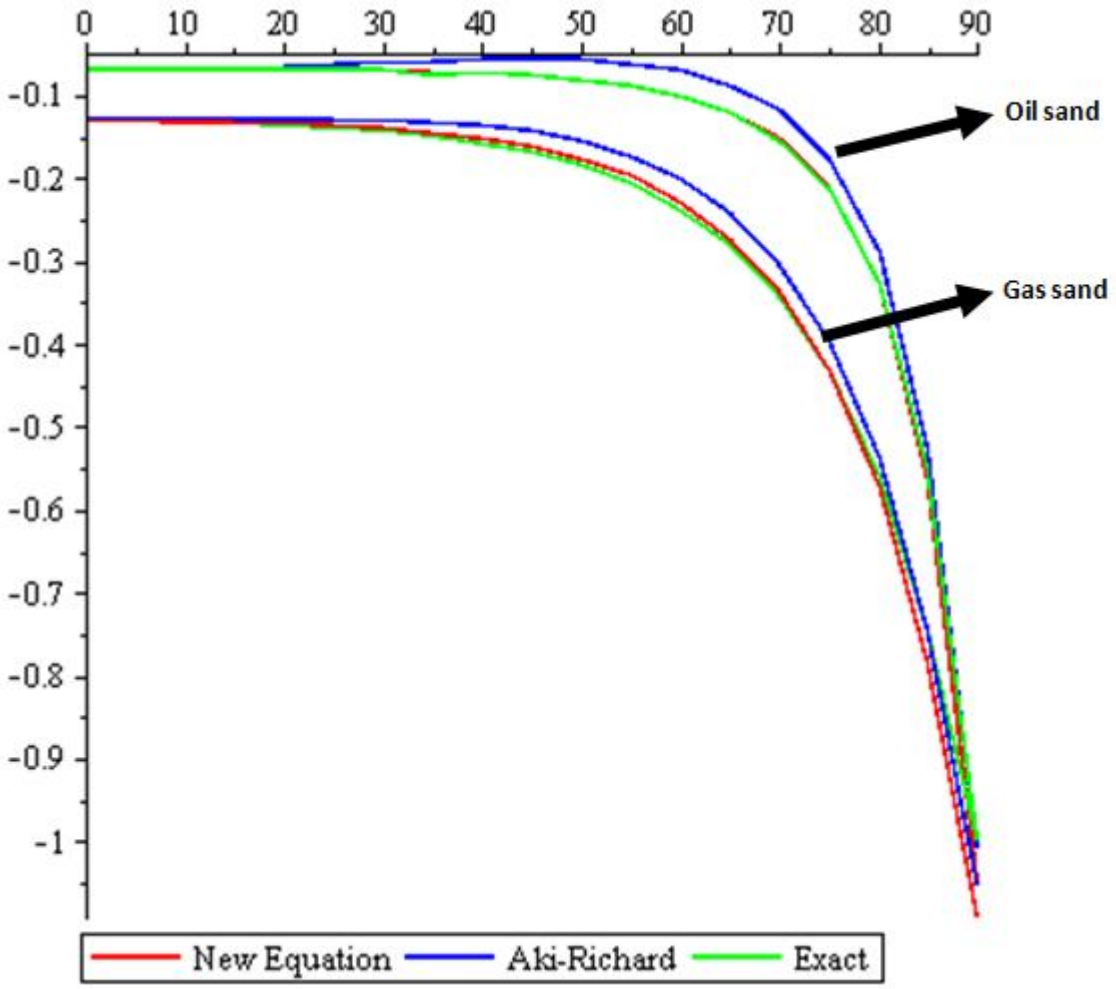

Fig. 6. Comparison of angle reflection coefficients, $R_{PP}(\theta)$obtained from Exact Zoeppritz equation, Aki-Richards and the modified Zoeppritz approximation for Class III Shale over Gas sand and Shale over Oil sand for a range of incidence angles from 0 to 90^0

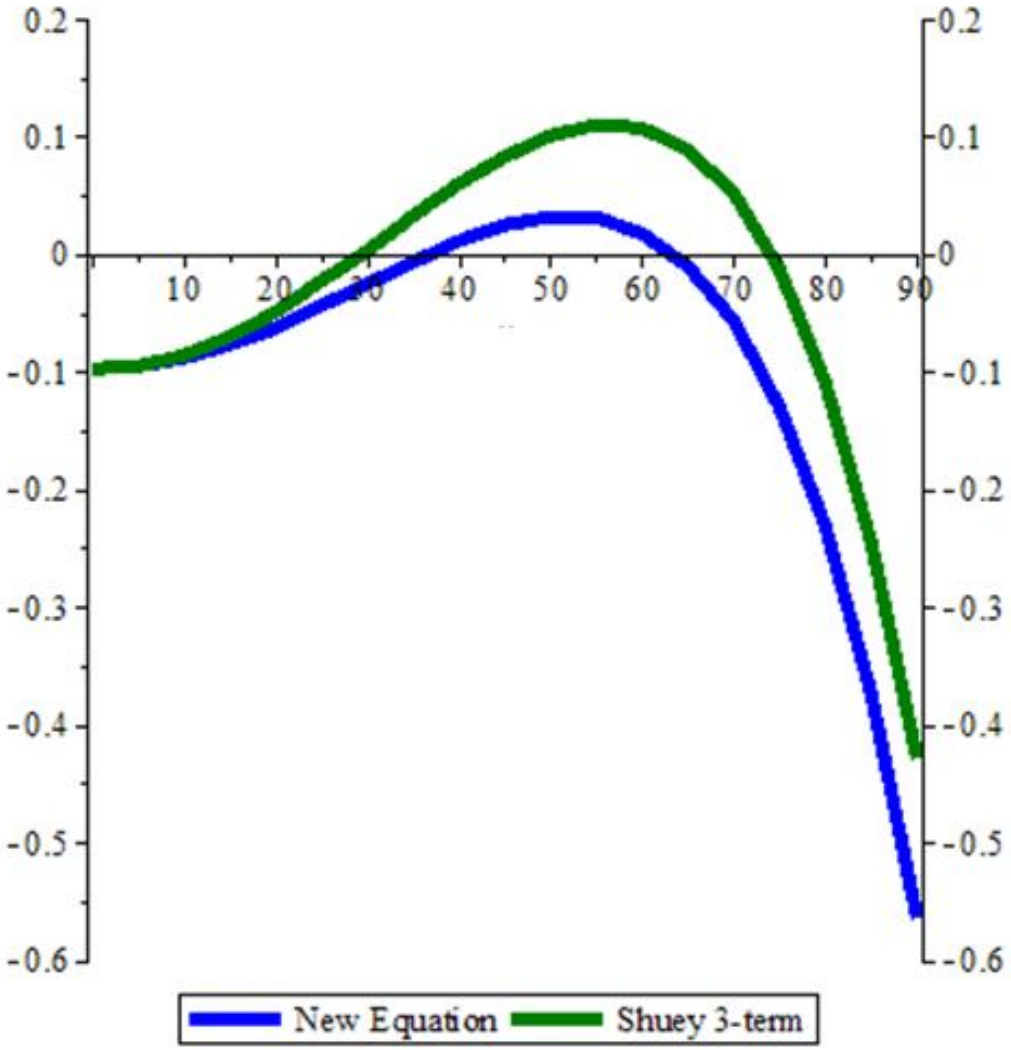

Fig.7. Comparison of angle reflection coefficient,$R_{PP}(\theta)$ obtained from the modified Zoeppritz approximationand Shuey's approximation for Class II Gas sand over Shale for a range of incidence andles from 0 to 90^0.

4. CONCLUSION

In this study, Zoeppritz equation have been modified and analyzed and their implication for hydrocarbon exploration in the Niger Delta Basin was investigated. This study shows a modification of the P – P wave reflectivity coefficients in form of Pseudo Poisson' ratio reflectivity($\Delta q/\mathrm{q}$), rigidity reflectivity ($\Delta\mu/\mu$), and density reflectivity ($\Delta\rho/\rho$)as a function of the fundamental elastic parameters of the subsurface. This modified equation has three terms like the Aki-Richard and Shuey (three terms) equations but is more stable and has higher accuracy at far offset (above the critical angle).

Reflectivity curves were generated from the Aki and Richards', Shuey's, modified Zoeppritz approximations and exact Zoeppritz equation in this study for the purposes of comparison

and validation of the results. Comparison of results for Class III AVO plot for shale over gas sand and shale over oil sand scenarios shows negative normal reflectivity amplitudeR_0response increases with increasing angle/offset was observed. The AVO plot of shale over gas sand response shows high negative zero-offset reflectivity at approximately –0.1311 than shale over oil sand response at –0.0703. This implies larger reflection amplitudes for shale over gas sand than shale over oil sand.The plot shows that Zoeppritz's equation, Aki and Richard's approximation and the modified equation fit each other near the critical angle25° while that of Zoeppritz and the modified equation, fit well beyond 25°. This could be attributed to the sensitivity of the elastic parameters in the modified equation which are fractional contrast of Pseudo Poisson' ratio reflectivity ($\Delta q/\mathrm{q}$), rigidity reflectivity ($\Delta\mu/\mu$), and density reflectivity ($\Delta\rho/\rho$).

For the Class II AVO plot, the reflection coefficient is slightly negative a zero offset and becomes less negative as the offset increases for gas over shale reflectivity generated from Shuey's approximation with a phase change at less than 30°angle of incidence while the modified equation has a phase change at less than 40° angle of incidence.Shuey's approximation breaks down before the critical angle showing the inadequacy of the approximation while the modified equation is stable at angles above the critical angle 30°. This indicates that the modified equation can be applied in exploration beyond the critical angle than the shuey's approximation especially for deep targets and wide angle acquisition for accurate estimation of intercept and gradient attributes.The modified equation has reflectivity at increasing angle of incidence $R(\theta)$ slightly less negative than Shuey's approximation. Shuey's approximation is best at incident angle less than 30°, while the new approximation is best at incident angle less than 60° before the second phase reversal

In conclusion, the results show that the Aki and Richards' and Shuey's approximations agrees with the exact equation up to the critical angle and also with the modified Zoeppritz equation. While only the exact Zoeppritz and the modified equation agrees well beyond the critical anlge. Therefore the modified Zoeppritz approximationgives higher accuracy at far offset than the two foremost approximationsand this is due to the sensitivity of the elastic parameters in the derived equation.

REFERENCES

Mahmoudian F, Margrave GF.P-wave impedance, S-wave impedance and density from linearAVO inversion: Application to VSP data from Alberta. CREWES Research Report. 18; 2006

Feng H, Bancroft JC. AVO principles, processing and inversion CREWES Research Report — 18; 2006

Bortfeld R. Approximations to the reflection and transmission coefficients of plane longitudinal and transverse waves: Geophysical Prospecting. 1961;9:485-502.

Aki KI, Richards PG. Quantitative seismology - Theory and methods,W. H. Freeman and Company, San Francisco. I, 5.2; 1980

Shuey RT. A simplification of the Zoeppritz Equations: Geophysics.1985;50:609 – 614.

Feng H. Hydrocarbon indicators derived from AVO analysis (Master Thesis).University of Calgary, Canada. 2009

Smith GC, Gidlow PM. Weighted stacking for rock property estimation and detection of gas: Geophysical Prospecting. 1987;35:993-1014.

Larsen JA. AVO Inversion by Simultaneous P-P and P-S Inversion (Masters Thesis), University of Calgary, Canada.Consortium for Research in Elastic Wave Exploration Seismology. 1999

Fatti JL, Smith GC, Vail PJ, Strauss PJ, Levitt PR. Detection of gas in sandstone reservoirs using AVO analysis: A 3-D seismic case history using the Geostack technique: Geophysics. 1994;59:1362-1376.

Goodway W, Chen T, Downton J. Improved AVO Fluid detection and lithology discrimination using lame petrophysical parameters, from P- and S- inversion. CSEG. 1997;148-151.

Hilterman F, Verm R. Lithology color-coded seismic sections: The calibration of AVO cross-plotting to rock properties. The Leading Edge. 1995;14(8):847-853.

Gray D, Goodway W, Chen T. Bridging the gap: Using AVO to detect changes in fundamental elastic constants: SEG meeting abstracts. 1999;852-855.

Samba CP, Jiangping L.The Direct Inversion of $\lambda/\mu$from Elastic Impedance. Journal of American Science. 2011;7(3):317-321.

Mavko G, Mukerji T, Dvorkin J. The Handbook of Rock Physics.Cambridge University Press.United Kingdom;1998.

Castagna JP, Backus MM. AVO analysis-tutorial and review, in Castagna, J. P and Backus MM., eds, Offset-dependent reflectivity. Theory and practice of AVO analysis: Society of Exploration Geophysicists. 1993;3 – 37.

Ganssle G.Calculation of a Synthetic Gather using the Aki-Richards Approximation to the Zoeppritz Equations. University of New Orleans Theses and Dissertations;2012.

Jalali V. Seismic AVO Attributes and Rock Physics in Hydrocarbon Exploration (Masters Thesis). Eastern Mediterranean University Gazimağusa, North Cyprus; 2014.

Richards PG, Frasier CW. Scattering of elastic waves from depth-dependent inhomogeneties.Geophysics. 1976;41: 441-458.

Lu Q, Song C, Liu C. A new prestack three-parameter amplitude variation with offset inversion method. Journal of Geophysics and Engineering. 2018;15:1300–1309

Castagna JP, Batzle ML, Kan TK. Rock physics – the link between rock properties and AVO response. In Offset Dependent Reflectivity – Theory and Practice of AVO Analysis (eds. J. P. Castagna and M. M. Backus) Tulsa: SEG. 1993.

Xu Y. AVO developments applied to Blackfoot 3C-2D broadband line (Master's Thesis). University of Calgary, Canada.Consortium for Research in Elastic Wave Exploration Seismology; 1999.

Sheriff RE, Geldart L P. Exploration seismology. Cambridge university press; 1995.

Rosa ALR. Análise do sinal sísmico. Sociedade Brasileira de Geofísica, Rio de Janeiro. 2018;713.

Yilmaz Ö. Seismic data analysis: Processing, inversion, and interpretation of seismic data. Society of exploration geophysicists; 2001.

Castagna JP, Swan HW, Foster DJ. Framework for AVO gradient and intercept interpretation. Geophysics. 1998;63:948–956.

Russell BH, Hampson D, Bankhead B. An Inversion Primer, CSEG Reorder, Special Edition.2006; 96-103.

Short KC, Stauble AJ. Outline of geology of Niger Delta: American Association of Petroleum Geologists Bulletin. 1967;51:761 – 779.

Turtle MLW, Charpentier RR, Brownfield ME. The Niger Delta Petroleum System: Niger Delta Province, Nigeria, Cameroun, and Equatorial Guinea, Africa. U.S.G.S. Open file Report. 1999;50 – 54

Corredor F, Shaw JH, Bilotti F. Structural styles in the deep-water fold and thrust belts of the Niger Delta: American Association of Petroleum Geologists Bulletin. 2005;89:753 – 780.

Itamuko OJ. 3D Seismic Structural Interpretation and Petrophysical Evaluation of 'X'-Field, Niger Delta Basin, Nigeria (B. Tech.).Federal University of Technology, Akure, Nigeria. . 2008.

Doust H, Omatsola E. Niger Delta, in J.D. Edwards, and P.A. Santogrossi, Divergent/passive margin basins: American Association of Petroleum Geologists Memoir. 1990;48: 201 – 238.

Shannon PM, Naylor N. Petroleum Basin Studies: London, Graham and Trotman Limited. 1989;153-169.

Heinio P, Davies RJ. Degradation of compressional fold belts: Deep-water Niger Delta: AAPG Bulletin. . 2006;90:753 – 770.

Odumodu CFR, Ezeh MO. Weathered Layer Delineation in an 'X' Field in the Niger Delta Basin of Nigeria: The Uphole Data Acquisition Technique. Journal of Earth Sciences and Geotechnical Engineering. 2014;3:115-130

Edohor EH, Balogun AO.Petrophysical Evaluation of H-field, Onshore Niger Delta Sedimentary Basin, Nigeria.Asian Journal of Geological Research. 2020;3(2):1-16.

Google Earth. Image Landsat/Copernicus. 2018.

Lawrence SR, Munday S, Bray R. Regional geology and geophysics of the eastern Gulf of Guinea (Niger Delta to Rio Muni): The Leading Edge. 2002;21(11):1112–1117.

Pengyuan S, Xiuli L, Yanpeng L, Yuanyuan Y. Haifeng C. Elastic parameter AVO approximations and their applications: BGP, CNPC SEG Las Vegas Annual Meeting. 2008;523-527.

Almutlaq MH, Margrave GF. Tutorial: AVO inversion, CREWES Research Report — 22. 2010

Ma J, Morozov IB. Ray-path elastic impedance, CSEG National Convention Great Explorations – Canada and Beyond. 2004;10-12.

Balogun AO, Ebeniro JO.Evaluation of Seismic Attributes Generated from Extended Elastic Impedance for Lithology and Fluid Discrimination, International Journal of Science and Research (IJSR). 2017;6(9):776 – 779.

Balogun AO, Ehirim CN.Lithology and Fluid Discrimination Using Bulk Modulus and Mu-Rho Attributes Generated From Extended Elastic Impedance, International Journal of Science and Research (IJSR). 2017;6(10):639 – 643.